Spine

Mandip K. Heir, Amit Shah, and Winston J. Rennie

Spine

When the paediatric spine develops, important morphological and biomechanical changes occur, during the synchronised growth of the vertebral bodies, posterior arches, spinal cord and roots [1].

Vertebrae formed as somites derived from paraxial mesoderm at 3 weeks of gestational age begin to surround the neural tube and notochord, forming a sclerotome. These sclerotome cells on either side of the cord migrate around the cord merging together at 4 weeks of gestational age. Segmentation of these sclerotomes forms the vertebral bodies [2].

M. K. Heir (✉)
Leicester Royal Infirmary, Infirmary Square, Leicester, UK
e-mail: mandip.heir@uhl-tr.nhs.uk

A. Shah
Leicester Royal Infirmary, Infirmary Square, Leicester, UK
e-mail: amit.shah2@nhs.net

W. J. Rennie
Leicester Royal Infirmary, Infirmary Square, Leicester, UK

Loughborough University, Loughborough, UK
e-mail: winston.rennie@uhl-tr.nhs.uk

P. Simoni, M. P. Aparisi Gómez (eds.), *Essential Measurements in Pediatric Musculoskeletal Imaging*,
https://doi.org/10.1007/978-3-031-17735-4_3

Chondrogenesis and then endochondral ossification of the vertebral bodies start at 40–60 days gestational age, with ossification continuing up to 25 years of age [3]. The three primary ossification centres are the vertebral body and bilateral neural ossification centres forming a neurocentral synchondrosis, contributing to vertebral body, spinal canal and posterior element development. Five secondary ossification centres include the superior and inferior surfaces of the vertebral body, transverse process tips and spinous process tip.

At term the oval ossified nucleus of the vertebral body is small relative to the large cartilaginous endplates, with unfused neurocentral synchondrosis. The neurocentral synchondrosis closes at different ages within the cervical, thoracic and lumbar spine, up to the age of 17 years [4]. As the ossification of the vertebral bodies and posterior elements completes, the spinal canal diameter reduces.

Cervical spine curvature is present in utero, secondary to head weight and uterine constraints [5]. The primary curves of the spine at birth are the thoracic and sacral curves. Biomechanical changes when able to hold the head and when able to weightbear result in the normal cervical and lumbar lordosis curvatures of the spine [2]. By the age of 10 years, the spinal curvature is similar to an adult, although absence of cervical lordosis can be seen up to the age of 16 years [6].

Cervical Spine

Basilar Invagination/Impression

Basilar impression is the upward displacement of the vertebral elements with normal bone, into a normal foramen magnum. Basilar invagination is similar upward displacement due to pathology of the bones [7]:

- Chamberlain line (Fig. 1): Line drawn from posterior margin of the hard palate to opisthion (posterior margin of the foramen magnum). Tip of odontoid process should normally be <2.5 mm above this line. If the odontoid process

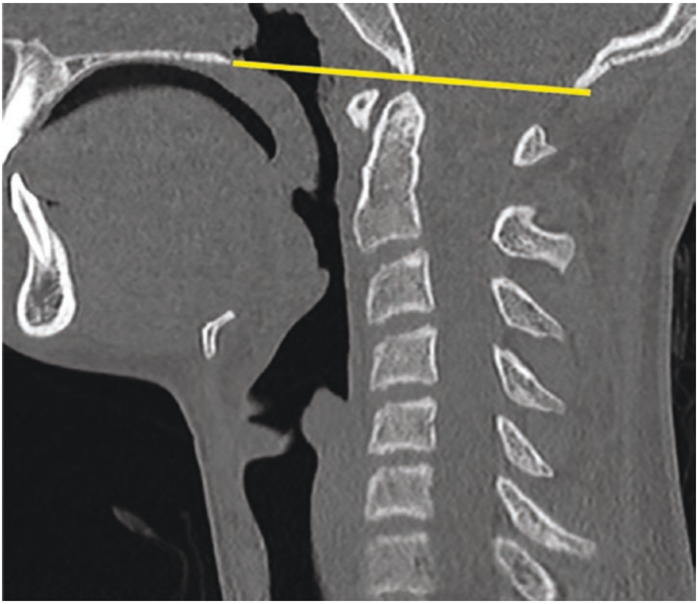

Figure 1 A sagittal CT image demonstrating the Chamberlain line

tip is >2.5 mm above the line, there is basilar invagination [8]. However, using this criterion alone to diagnose basilar invagination may lead to high false positives [9].

- Clivodens angle (Fig. 2): Angle formed when line drawn along long axis of clivus and long axis of dens. A value of <125° suggests basilar invagination [9].

Atlanto-Occipital Junction

- Basion-dens interval in assessing atlanto-occipital dislocation (Fig. 3): Distance between the basion and the odontoid process of C2 should be 12 mm or less [6]. This measurement should be used cautiously in children as the odontoid height increases with age in normal development. Under 9 years of age, the odontoid is shorter than the level of the anterior arch of C1 height [10].

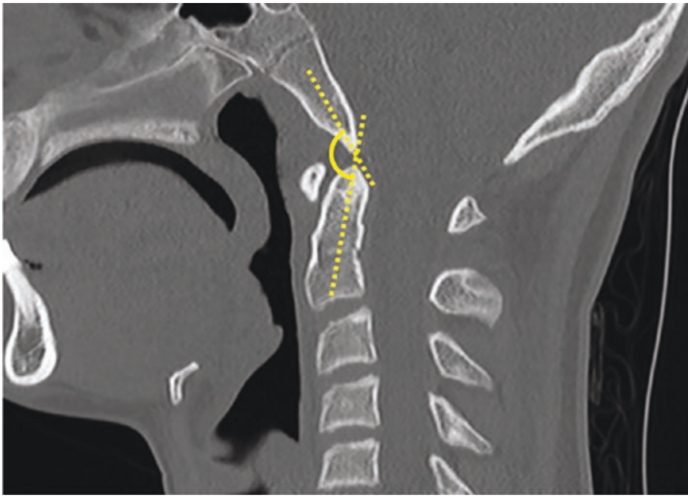

FIGURE 2 A sagittal CT image demonstrating the Clivodens angle

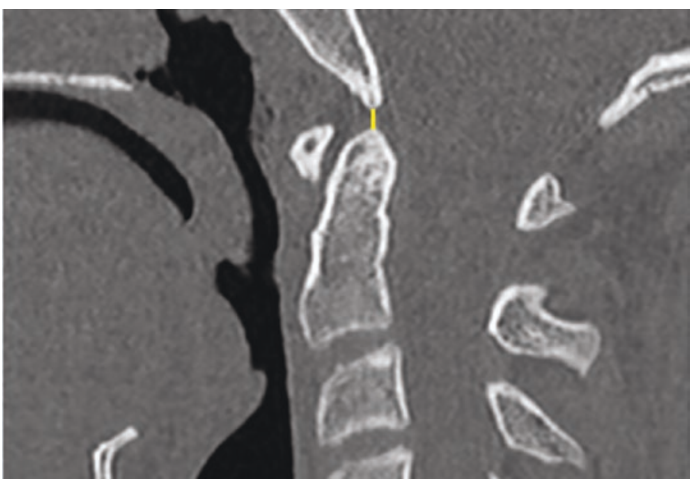

FIGURE 3 A sagittal CT image demonstrating the basion-dens interval

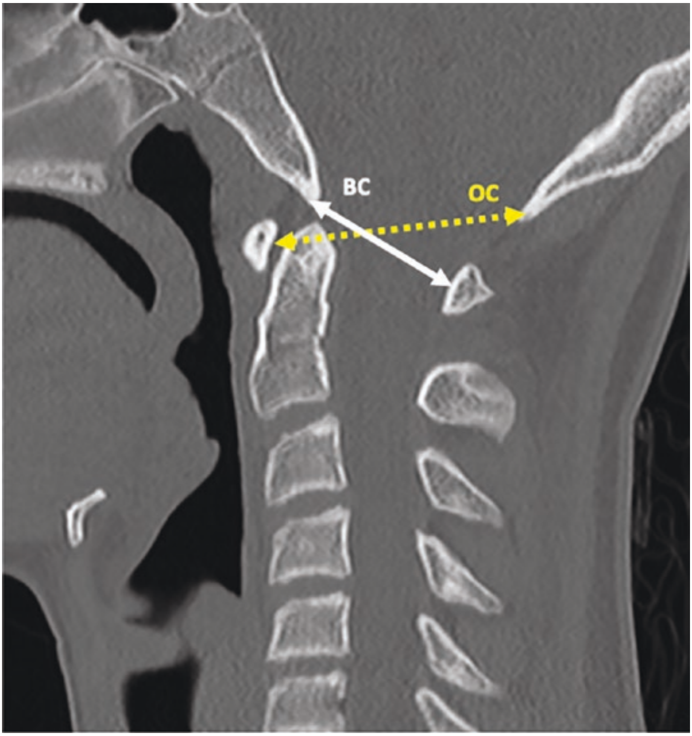

FIGURE 4 A sagittal CT image demonstrating the lines drawn to calculate Powers ratio (BC/OC). *BC:* basion to posterior C1 (in white) and *OC:* ophistion to anterior C1 (in dotted yellow)

- Powers ratio to detect subluxation/dislocation (Fig. 4): Distance from the tip of the basion to the posterior arch of C1 (BC) divided by the distance from the opisthion to the anterior arch of C1 (OC). A Powers ratio (BC/OC) of less than 1 is considered standard on radiographs. On CT, a ratio of less than 0.9 (midline sagittal plane) is considered standard. A Powers ratio (BC/OC) of more than 1 on flexion and extension views is diagnostic of anterior atlanto-occipital instability [11].

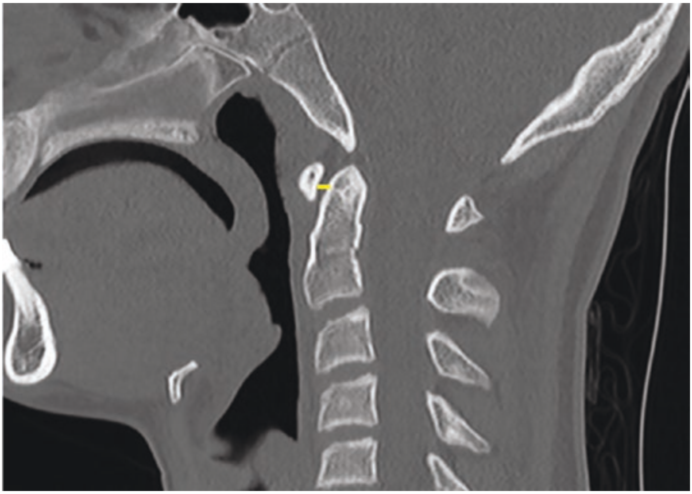

FIGURE 5 A sagittal CT image demonstrating the atlanto-dens interval

Atlanto-Dens Interval (ADI)

This is an important measurement when assessing atlanto-axial subluxation. The ADI is measured between the posteroinferior margin of the anterior arch of the atlas and the anterior surface of the odontoid process (Fig. 5). Extension/flexion of the cervical spine during positioning can affect ADI measurement; hence, ADI should be measured in neutral position [12]. Normal values in neutral position are <4 mm in children <9 years of age and <3 mm in children >9 years age [13].

Posterior Atlanto-Dens Relationship

If a posterior ligamentous injury is suspected on lateral X-rays performed in flexion, the posterior atlanto-dens relationship can be assessed. The ratio between the posterior arch

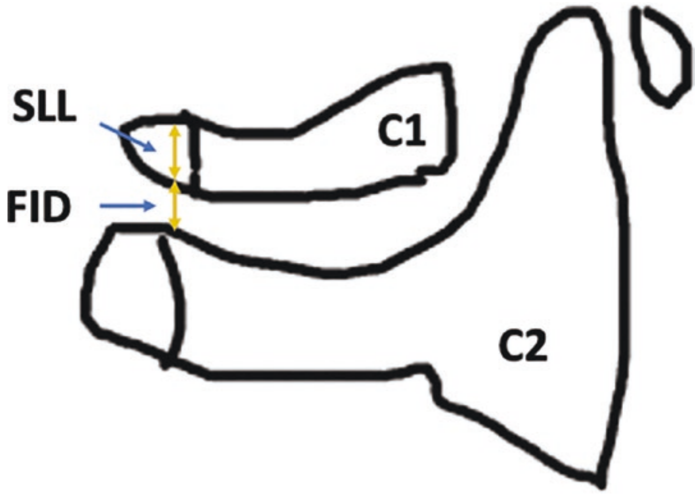

FIGURE 6 A diagram demonstrating the spinolaminar line (SLL) and flexion interspinous distance (FID)

of C1 at the spinolaminar line (SLL) and the interspinous distance between C1 and C2 (FID) in flexion is calculated (Fig. 6). FID/SLL >2 suggests a posterior ligamentous injury in all ages [14].

Posterior Cervical Line/Posterior Line of Swischuk

Anterior displacement of C2 on C3 has been observed in children up to the age of 7 years [15]. The posterior cervical (Swischuk) line (Fig. 7) helps differentiate physiological displacement/pseudosubluxation from pathological subluxation. The posterior cervical/Swischuk line is drawn through the anterior cortex of the posterior arches of C1–C3.

In pathological subluxation, the line will miss the posterior arch of C2 by more than 2 mm [15] (Fig. 8).

Figure 7 A lateral X-ray demonstrating the posterior cervical line/ posterior line of Swischuk

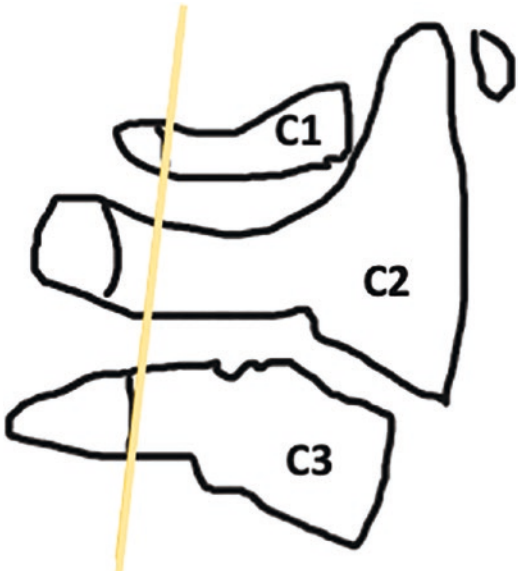

Figure 8 A diagram demonstrating pathological subluxation of C2 in relation to C3

Prevertebral Soft Tissue Assessment

- The prevertebral soft tissue thickness aids in the detection of cervical spine injuries. Thickness can be measured on both lateral cervical spine X-ray and sagittal CT, at C2 and C6 levels (Fig. 9), given the reduced variability in the measurements at these levels (Table 1).

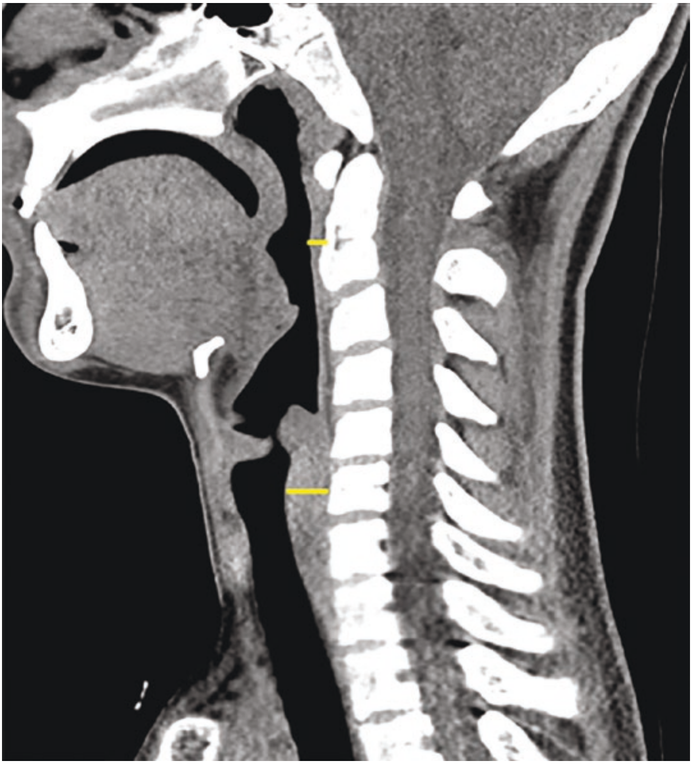

FIGURE 9 A sagittal CT image demonstrating the prevertebral soft tissue thickness at C2 and C6 vertebral levels

TABLE 1 Mean values of prevertebral soft tissue thickness at C2 and C6 levels, measured on MDCT [16]

Age (years)	Mean prevertebral soft tissue thickness at C2 (mm) mean ± SD	Mean prevertebral soft tissue thickness at C6 (mm) mean ± SD
0–2	5.0 ± 1.3	6.3 ± 1.4
3–6	5.0 ± 1.7	7.5 ± 1.2
7–10	4.6 ± 1.1	9.1 ± 1.5
11–15	4.6 ± 1.1	10.9 ± 1.8
18 years plus	3.7 ± 1.2	13.0 ± 2.6

Spinal Canal Size

After the age of 4 years, only minimal growth of the spinal canal diameter occurs, increasing on average 3.2 mm at C2 and 2.6 mm at C7 in males and 2.8 mm and 2.0 mm in females, respectively (Table 2) [17].

Vertebral Body Height

Cervical vertebral body height increases with age and growth, as well as changing from an oval morphology to rectangular (Table 3).

TABLE 2 Cervical spine canal AP dimension at C2 and C7 (modified from [17])

	Male		**Female**	
Age (years)	**C2 diameter (mm) mean ± SD**	**C7 diameter (mm) mean ± SD**	**C2 diameter (mm) mean ± SD**	**C7 diameter (mm) mean ± SD**
1	14.41 ± 1.23	13.35 ± 1.35	13.53 ± 1.28	12.56 ± 0.89
4	16.23 ± 1.05	14.91 ± 0.94	15.30 ± 1.59	14.56 ± 0.90
9	16.99 ± 1.21	15.06 ± 1.18	16.12 ± 1.00	14.12 ± 0.85
15	15.70 ± 1.43	14.53 ± 1.17	15.61 ± 1.67	14.15 ± 1.06

TABLE 3 Cervical body height at C3 and C5 (modified from [18])

	Male		**Female**	
Age (years)	**C3 vertebral body height (mm) mean ± SD**	**C5 vertebral body height (mm) mean ± SD**	**C3 vertebral body height (mm) mean ± SD**	**C5 vertebral body height (mm) mean ± SD**
0–5	5.52 ± 1.18	5.47 ± 1.19	5.84 ± 1.18	5.74 ± 1.12
5–10	7.82 ± 1.29	7.53 ± 0.99	8.09 ± 1.20	7.69 ± 1.10
10–15	11.51 ± 2.45	10.51 ± 2.10	11.56 ± 2.69	10.79 ± 2.16

Thoracolumbar Spine

Thoracic Kyphosis

- The spine has characteristic alignment in the coronal and sagittal planes. In the sagittal plane, the spine is lordotic in the cervical and lumbar regions and kyphotic in the thoracic region.
- The thoracic kyphosis angle increases with age and the increase is greater in females than in males.
- Kyphosis is a marked curvature of the spine in the sagittal plane, with a posterior convexity.
- According to the Scoliosis Research Society classification system, the curvature in the sagittal plane is normally smooth and comprised between 20° and 45°.

Modified Cobb Angle

- The upper (commonly T4/5) and lower (commonly T12) vertebral bodies defining the curve are selected and lines are drawn, extending along the superior border of the upper end vertebra as well as along the inferior border of the lower end vertebra. Perpendicular lines are drawn from these and the angle is measured at the intersection (most modern PACS systems will have angle tools that measure directly as in Fig. 10).

Sagittal Balance

- Essential for the spine body to maintain equilibrium. Alterations affect forces and energy required to maintain a horizontal gaze in the upright position.
- Sagittal balance is evaluated by measuring the distance between the posterosuperior aspect of the S1 vertebral body and the plumb line.

Figure 10 A lateral X-ray demonstrating modified Cobb angle measurement

C7 Plumb Line

- The plumb line is a vertical line drawn downwards from the centre of the C7 vertebral body, parallel to the lateral edges of the radiograph (Fig. 11).
- This line should pass through the superior endplate of S1, ± 2 cm of the posterosuperior corner of the S1 vertebral body [19, 20].

Figure 11 A lateral X-ray demonstrating the C7 plumb line

- The position of this line is can be positive, neutral or negative:
  - Positive balance: the plumb line passes more than 2 cm in front of the posterosuperior corner of the S1 vertebral body.
  - Neutral balance: the plumb line passes within 2 cm of the posterosuperior corner of the S1 vertebral body.
  - Negative balance: the plumb line passes more than 2 cm behind the posterosuperior corner of the S1 vertebral body.

Scoliosis

- Represents the presence of one or more lateral curves of the vertebral column in the coronal plane.

- Scoliosis is defined as a lateral spinal curvature with a Cobb angle of >10°.
- The Scoliosis Research Society classifies paediatric scoliosis as [21]:
  - Infantile 0–3.
  - Juvenile 4–10.
  - Adolescent 11–18.

Infantile Idiopathic Scoliosis

- 1.5× more frequent in boys than girls.
- 76% of cases scoliosis is left convex.
- Many infants with infantile idiopathic scoliosis are healthy and normal and simply have a small curvature of the spine. In some patients, however, there is an increased association with hip dysplasia, mental retardation and congenital heart disease.
- Many infantile curves will resolve without treatment.

Juvenile Idiopathic Scoliosis

- 10–15% of all idiopathic scoliosis in children.
- Early years, boys are affected slightly more than girls and the curve is often left-sided.
- Later years, predominance of girls and right-sided curves.
- As a rule of thumb, about 20% of children who are younger than 10 and who have a curve greater than 20° will have an underlying spinal condition (particularly an Arnold-Chiari malformation).
- Juvenile curves that reach 25–30° tend to continue to worsen without treatment.

Cobb Angle

- Lines are drawn along the endplates of the *terminale vertebrae*, and the angle between the two lines, where they intersect, is measured.
- The *cephalad* and *caudal terminale vertebra* are those vertebrae whose endplates are most tilted towards each other

(most modern PACS systems will have angle tools that measure directly as in Fig. 12).

- Mild 10–15°.
- Moderate 20–40°.
- Severe >40°.

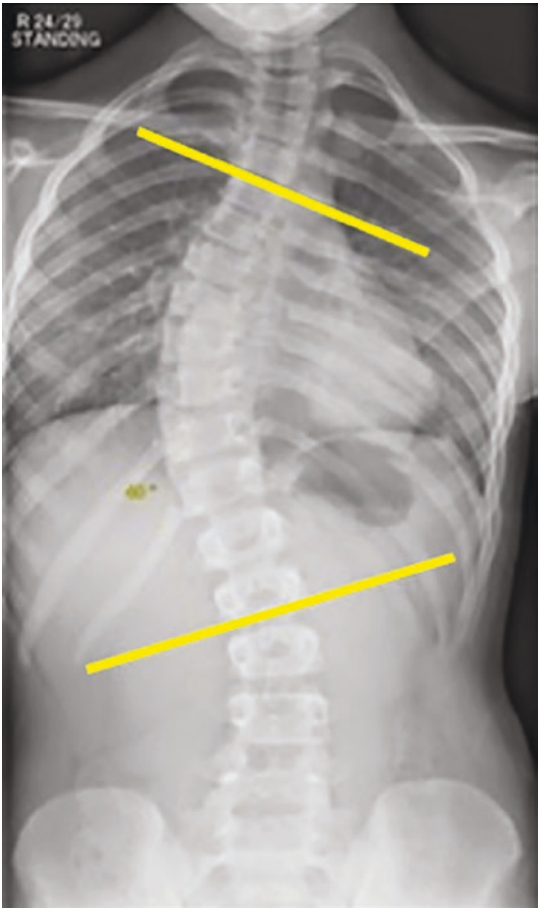

FIGURE 12 An anteroposterior X-ray demonstrating the Cobb angle

Coronal Balance

- Coronal balance is evaluated by measuring the distance between the central sacral vertical line (CSVL) and the plumb line.
- It measures whether or not the upper spine is located over the midline (normal) or off to one side.
- The CSVL is a vertical line that is drawn perpendicular to an imaginary tangential line drawn across the top of the iliac crests on radiographs. It bisects the sacrum.
- The plumb line is a vertical line drawn downwards from the centre of the C7 vertebral body, parallel to the lateral edges of the radiograph.
- The horizontal distance between this plumb line and the CSVL is measured (Fig. 13).
- The position of this line can then termed positive, neutral or negative, depending on distance and direction from the midline:
  - Positive balance: the plumb line passes to the right of the midline, by >2 cm.
  - Neutral balance: the plumb line passes within 2 cm of the midline.
  - Negative balance: the plumb line passes to the left of the midline, by >2 cm.

Lumbar Spinal Canal Dimensions

- Anteroposterior spinal canal development is fully complete by 5 years of age, while transverse spinal canal diameter increases until 15–17 years [22, 23].
- Considerable variation in the developmental size of the normal lumbar spinal canal exists within and between populations.
- The sagittal diameter is the shortest midline perpendicular distance from the vertebral body to the inner surface of the neural arch (Table 4) [24].

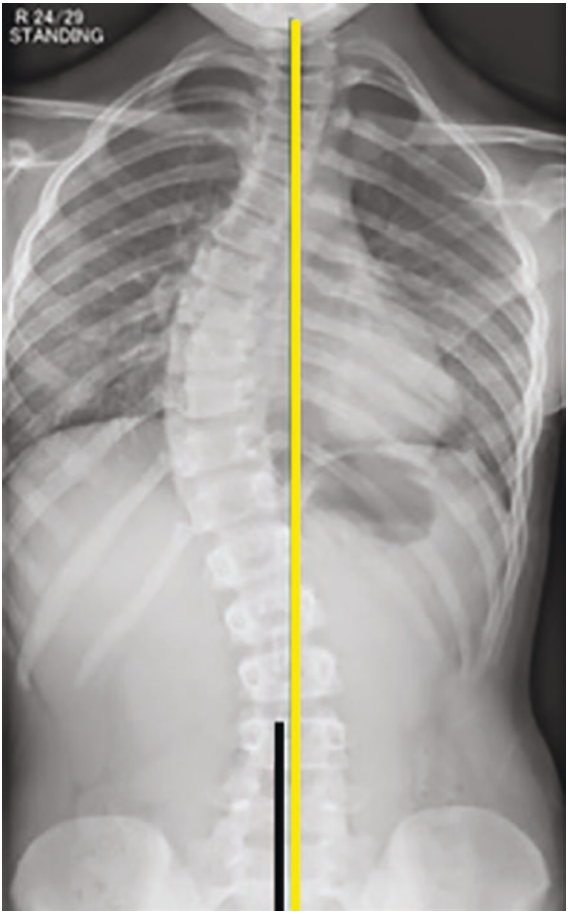

FIGURE 13 An anteroposterior X-ray demonstrating coronal balance (short black line is the CSVL and yellow line is the plumb line)

TABLE 4 Radiographic spinal canal dimensions [24]

	Spinal canal dimensions (mm) minimum-maximum				
Age (years)	**L1**	**L2**	**L3**	**L4**	**L5**
3–5	16–24	16–24	15–22	15–22	15–22
6–8	15–25	15–25	14–24	14–24	14–24
9–10	16–24	16–24	15–23	15–23	15–23
11–12	15–26	14–25	14–24	14–24	15–25
13–14	17–24	17–23	16–22	13–28	13–28
15–16	16–24	16–24	15–23	15–23	15–23
17–18	16–28	16–28	16–28	16–28	16–28

- Knirsch et al. measured the sagittal diameters of the lumbar spine (vertebral body and dural sac) on MRI in 75 healthy children (32 boys, 43 girls) between 6 years and 17 years of age (Table 5).
- Measurements are made perpendicular to the long axis of the vertebral body and the dural sac (Fig. 14). The dural sac dimension (DSD) was measured as the longest distance between the posterior border of the vertebral body and the anterior border of the spinous process.

TABLE 5 MRI spinal canal dimensions in mm [25]

Age (years)	MRI spinal canal dimensions (mm) mean ± SD					
	L1	L2	L3	L4	L5	S1
6–8	16.1 ± 1.8	15.6 ± 1.5	14.5 ± 1.4	14.1 ± 1.3	15.1 ± 2.1	13.7 ± 1.7
9–11	17.1 ± 1.3	16.1 ± 1.1	15.6 ± 1.5	15.7 ± 1.9	15.9 ± 1.2	14.6 ± 2.0
12–14	17.7 ± 1.9	16.7 ± 1.8	16.2 ± 1.7	16.7 ± 1.9	16.9 ± 2.4	14.7 ± 2.9
15–17	17.6 ± 1.8	16.4 ± 1.8	15.5 ± 1.5	16.4 ± 1.6	17.4 ± 2.3	15.0 ± 2.5

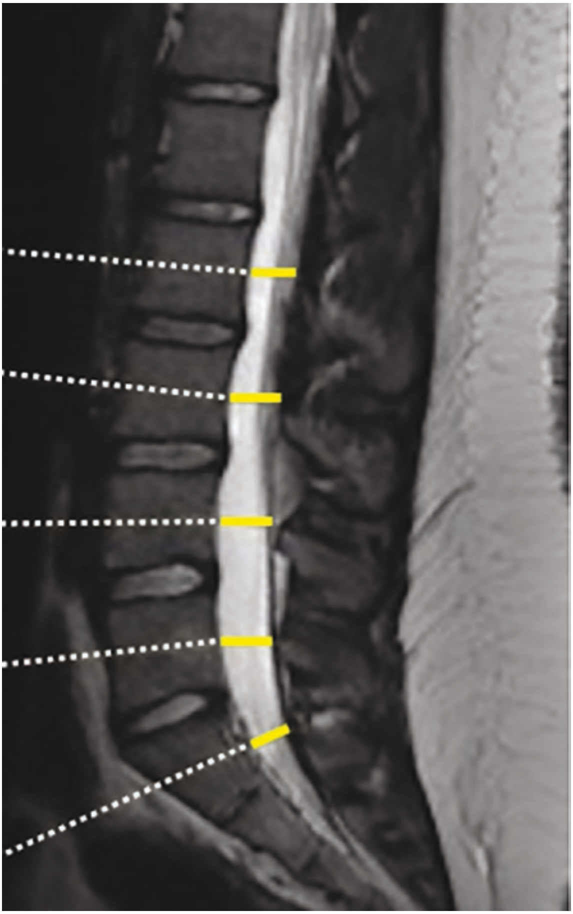

FIGURE 14 A sagittal T2 MR image demonstrating spinal canal dimension measurements

References

1. Raimondi AJ, Choux M, Di Rocco C. The paediatric spine I: development and the Dysraphic state. New York: Springer-Verlag; 1989. p. 39–40. (A DiMeglio and F Bonnel. Chapter 3 Growth of the spine pages 39-40).

2. Aparisi Gomez MP, Watkin S, Perry D, et al. Anatomical considerations of embryology and development of the musculoskeletal system: basic notions for musculoskeletal radiologists. Semin Musculoskelet Radiol. 2021;25:3–21. https://doi.org/10.1055/s-0041-1723005.
3. Colafati GS, Marrazzo A, Marco C, et al. The paediatric spine. Semin Musculoskelet Radiol. 2021;25:137–54. https://doi.org/10.1055/s-0041-1727095.
4. Blakemore L, Schwend R, Akbarnia BA, Dumas M, Schmidt J. Growth patterns of the neurocentral synchondrosis (NCS) in immature cadaveric vertebra. J Pediatr Orthop. 2018;38(3):181–4. https://doi.org/10.1097/BPO.0000000000000781.
5. Abelin-Genevois K, Idjerouidene A, Roussouly P, et al. Cervical spine alignment in the paediatric population a radiographic normative study of 150 asymptomatic patients. Eur Spine J. 2014;23:1442–8.
6. Lustrin ES, Karakas SP, Ortiz AO, et al. Pediatric cervical spine: normal anatomy, variants and trauma. Radiographics. 2003;23:539–60.
7. Cronin CG, Lohan DG, Ni Mhuircheartigh J, et al. MRI evaluation and measurement of the normal odontoid peg position. Clin Radiol. 2007;62:897–903.
8. Baysal B, Eser MB, Sorkun M. Radiological approach to basilar invagination type B: reliability and accuracy. J Neuroradiol. 2020;49:33–49. https://doi.org/10.1016/j.neurad.2020.08.005.
9. Xu S, Gong R. Clivodens angle: a new diagnostic method for basilar invagination at computed tomography. Spine. 2016;41(17):1365–71.
10. Elliott S. The odontoid process in children—is it hypoplastic? Clin Radiol. 1988;39:391–3.
11. Gaunt T, Mankad K, Calder A, Tan AP, Talenti G, Watson TA, Thompson D. Abnormalities of the craniovertebral junction in the paediatric population: a novel biomechanical approach. Clin Radiol. 2018;73:839–54. https://doi.org/10.1016/j.crad.2018.05.020.
12. Locke GR, Gardner JI, Van Epps EF. Atlas-dens interval (ADI) in children. Am J Radiol. 1966;97(1):135.
13. Kale SS, Ailawadhi P, Yerramneni VK, et al. Paediatric bony craniovertebral junction abnormalities: institutional experience of 10 years. J Paediatr Neurosci. 2011;6(Suppl1):S91–5.
14. Keats TE, Sistrom C. Atlas of radiological measurement. 7th ed. Philadelphia, PA: Harcourt Health Services; 2001. p. 141–2.

15. Ghanem I, Hage SE, Rachkidi R, et al. Pediatric cervical spine instability. J Child Orthop. 2008;2:71–84. https://doi.org/10.1007/s11832-008-0092-2.
16. Vermess D, Rojas CA, Shaheen F, Pinakpani R, Martinez CR. Normal pediatric prevertebral soft-tissue thickness on MDCT. Am J Roentgenol. 2012;199:W130–3.
17. Johnson KT, Al-Holou WN, Anderson RCE, et al. Morphometric analysis of the developing pediatric cervical spine. J Neurosurg Pediatr. 2016;18:377–89.
18. Wang JC, Nuccion SL, Feighan JE, et al. Growth and development of the pediatric cervical spine documented radiologically. J Bone Jt Surg. 2001;83(8):1212–8.
19. Kim H, Kim HS, Moon ES, Yoon CS, Chung TS, Song HT, Suh JS, Lee YH, Kim S. Scoliosis imaging: what radiologists should know. Radiographics. 2010;30(7):1823–42. https://doi.org/10.1148/rg.307105061.
20. Roussouly P, Nnadi C. Sagittal plane deformity: an overview of interpretation and management. Eur Spine J. 2010;19(11):1824–36. https://doi.org/10.1007/s00586-010-1476-9. Epub 2010 Jun 22
21. Society of Scoliosis Research. Conditions and treatment. 2022. https://www.srs.org/professionals/online-education-and-resources/conditions-and-treatments.
22. Papp T, Porter RW, Aspden RM. The growth of the lumbar vertebral canal. Spine. 1994;19:2770–3.
23. Watts R. Lumbar vertebral canal size in adults and children: observations from a skeletal sample from London, England. Homo. 2013;64:120–8.
24. Hinck VC, Hopkins CE, Clark WM. Sagittal diameter of the lumbar spinal canal in children and adults. Radiology. 1965;85(5):929–37.
25. Knirsch W, Kurtz C, Häffner N, Langer M, Kececioglu D. Normal values of the sagittal diameter of the lumbar spine (vertebral body and dural sac) in children measured by MRI. Pediatr Radiol. 2005;35(4):419–24. Epub 2005 Jan 6. https://doi.org/10.1007/s00247-004-1382-6.